



ELSEVIER

Journal of Alloys and Compounds 330–332 (2002) 162–165

Journal of  
ALLOYS  
AND COMPOUNDS

www.elsevier.com/locate/jallcom

# High pressure experiments on the $Mg_2Ni$ and $Mg_2NiH_4-H$ systems

J. Chen\*, T. Sakai, N. Kitamura, H. Tanaka, T. Kiyobayashi, H.T. Takeshita, N. Kuriyama

*Osaka National Research Institute, AIST, MITI, 1-8-31 Midorigaoka, Ikeda, Osaka 563-8577, Japan*

## Abstract

Electrical resistance of the  $Mg_2Ni$  and  $Mg_2NiH_4$  powders was measured under compressing up to 6 gigapascals (GPa), using the four-point probe method at 20°C. Effects induced by the high-pressure treatment and heating at 400°C with or without hydrogen source  $LiAlH_4$  were also studied. The structure and hydrogenation properties of the samples recovered after quenching from high pressure and high temperature were investigated employing the techniques of X-ray diffraction and thermal analyses such as differential scanning calorimetry, thermogravimetry and differential thermal analysis. Decreased absorption/desorption temperatures were observed for the treated samples owing to the changes of microstructure and kinetic factor. © 2002 Elsevier Science B.V. All rights reserved.

**Keywords:** High pressure;  $Mg_2Ni$  and  $Mg_2NiH_4-H$  system; X-ray diffraction; Thermal analysis

## 1. Introduction

The utilization of super high-pressure technology, which can reach the range of gigapascals (GPa), has made a great deal of progress in the experimental study of hydrogen storage materials [1–3]. It has demonstrated that such a high-pressure operation applied to a number of metal–hydrogen systems is an effective route to produce vacancies in the host metallic matrix, of which various novel properties can be expected [4–7]. High compaction pressures of up to 10 kbar (1 GPa) cause the transformation of the orthorhombic structure of  $Mg_2NiH_4$  into the monoclinic one, resulting in reduced decomposition temperatures attributing to kinetic factor [8]. Our recent study shows that the  $Mg_2NiH_4$  after high-pressure (6 GPa) and high temperature (600°C) treatment can desorb hydrogen at quite a low temperature owing to the instability of the sample [9].

The aim of this work is to clarify the compressing effects of the  $Mg_2Ni$  and  $Mg_2NiH_4-H$  systems on the structural and hydriding properties.

## 2. Experimental

The  $Mg_2Ni$  and  $Mg_2NiH_4$  powders, which were sup-

plied by JMC (Japan Metal & Chemical Co. Ltd.), were initially compressed into a hard-packed cylindrical pellet ( $\varnothing 5.0\text{ mm} \times 10.0\text{ mm}$ ) under an oil pressure of 4 ton  $\text{cm}^{-2}$ , and then placed in a high pressure cell that is shown in Fig. 1. The alloy  $Mg_2Ni$  contains a slight excess of free magnesium to prevent the formation of  $MgNi_2$  during the preparation, and then the hydride  $Mg_2NiH_4$  contains small amounts of  $MgH_2$ . The electrical resistance of the  $Mg_2Ni$  and  $Mg_2NiH_4$  was checked at 20°C by a four-point resistance measurement. The electrical resistivity was calculated from the pellet length and area. The hydrogen source  $LiAlH_4$  (Lithium Aluminiumhydrid) was purchased from Chemetall GmbH (Germany). The high-pressure cell assembly and treating were the same as that previously described in detail [4,9]. After recovery, the sample was

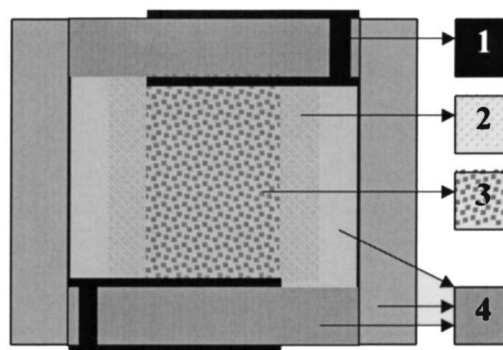


Fig. 1. Schematic diagram showing electrical resistance measurements during the compressing process: (1) copper, (2) NaCl, (3) sample, (4) pyrophyllite.

\*Corresponding author. Tel.: +81-727-519-651; fax: +81-727-519-629.

E-mail address: junchen@onri.go.jp (J. Chen).

carefully split into pieces and measured immediately by X-ray diffraction (XRD), differential scanning calorimetry (DSC), or thermogravimetry (TG) and differential thermal analyses (DTA). In XRD measurement experiments, samples were mixed with a protective coating of pyropllylite oil, smeared on a glass slide and exposed to monochromatic Cu-K $\alpha$  radiation using a RU-200 Rigaku X-ray Powder Diffractometer ( $\lambda=1.5406 \text{ \AA}$ ) operated at 40 kV with a current beam of 150 mA. The X-ray intensity was measured over a diffraction angle from 5 to 85° with a velocity of 0.02° per step and 2°/min. The DSC analysis was carried out employing a Rigaku Thermo-Plus DSC8230HP instrument, at 3.0 MPa hydrogen pressure and with a heating and cooling rate of 5°/min. The TG and DTA spectra were obtained with a Rigaku Thermo-Plus TG8120 apparatus. Samples were heated linearly from 30 to 400°C with a ramp of 5°C/min in a slow stream of argon. Aluminum oxide cups were used to hold the sample and alumina reference.

### 3. Results and discussion

#### 3.1. Electrical resistance

Fig. 2 shows the course of electrical resistance of the Mg<sub>2</sub>Ni and Mg<sub>2</sub>NiH<sub>4</sub> as a function of pressure. It can be seen that the Mg<sub>2</sub>NiH<sub>4</sub> exhibits large changes of the electrical resistance, whereas the Mg<sub>2</sub>Ni exhibits a rather slow decrease. The initial fast decreasing (less than 1 GPa) of electrical resistance results from mechanical changes of the samples due to the influence of pure hydrostatic pressure. The resistance drop of Mg<sub>2</sub>NiH<sub>4</sub> at about 1.2 GPa, which may be caused by mechanical change or by the insulator–conductor transformation, is not reversible dur-

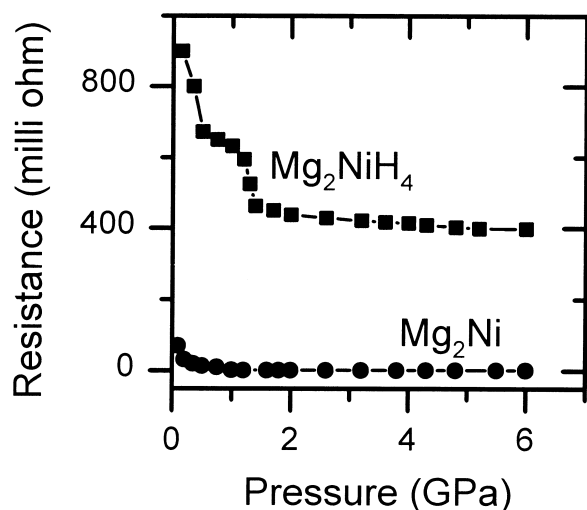


Fig. 2. Electrical resistance of the Mg<sub>2</sub>Ni and Mg<sub>2</sub>NiH<sub>4</sub> measured by the four-point method as a function of pressure at 20°C.

ing the pressure releasing process. At 6 GPa, the electrical resistances of the Mg<sub>2</sub>Ni and Mg<sub>2</sub>NiH<sub>4</sub> were 2 and 399 mΩ, respectively. Based on the diameter and length of the cylindrical pellets after compressing, the electrical resistivities of the nominal Mg<sub>2</sub>Ni and Mg<sub>2</sub>NiH<sub>4</sub> at 6 GPa were calculated to be 0.4 and 79.8 mΩ cm. These data are in agreement with the result reported previously by Gavra et al. [8] who observed the transition of Mg<sub>2</sub>NiH<sub>4</sub> from an insulating to a conducting material but with no specific conductivity.

#### 3.2. Effects of high-pressure of Mg<sub>2</sub>Ni on XRD and DSC

Fig. 3 presents the XRD patterns obtained for the recovered Mg<sub>2</sub>Ni along with a profile of untreated Mg<sub>2</sub>Ni for the comparison. In Mg<sub>2</sub>Ni untreated, the peaks, except that marked by down triangles owing to the coexistence of small amounts of Mg, all arise principally from the hexagonal host structure. In the case of as-treated Mg<sub>2</sub>Ni sample, in particular after recovery from 6 GPa with heating, it is observed that the peaks shift to higher angles showing a decrease in the unit cell constants of the treated Mg<sub>2</sub>Ni. At the same time, the full width of half-maximum intensity for all peaks is found larger (about 2 times) than that of Mg<sub>2</sub>Ni untreated, illustrating that the crystalline size of the as-treated sample becomes smaller or/and lattice deformation occurs [10]. Furthermore, the peaks of Mg were not observed in the treated samples, possibly owing to the diffusion of Mg atoms in the given treatment that results in a smaller grain size.

Fig. 4 indicates the high-pressure operation on the effect of the DSC characteristics. The DSC heating and cooling curves of untreated Mg<sub>2</sub>Ni exhibit sharp exothermic and endothermic peaks, attributing to the hydride formation

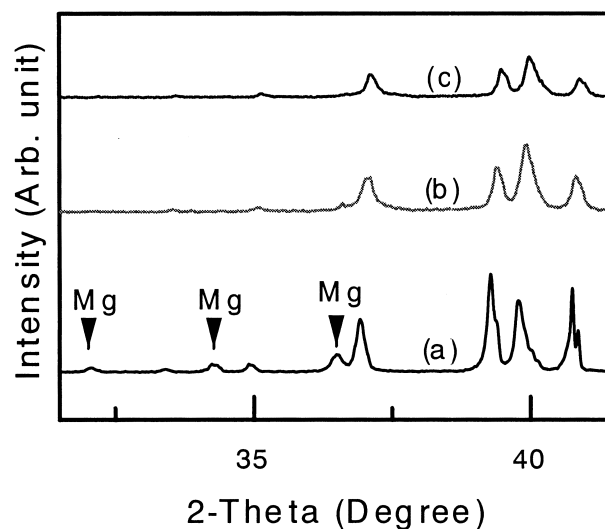


Fig. 3. X-ray diffraction (XRD) patterns of the Mg<sub>2</sub>Ni system: (a) initial alloy, and recovered from (b) 6 GPa, (c) 6 GPa and 400°C.

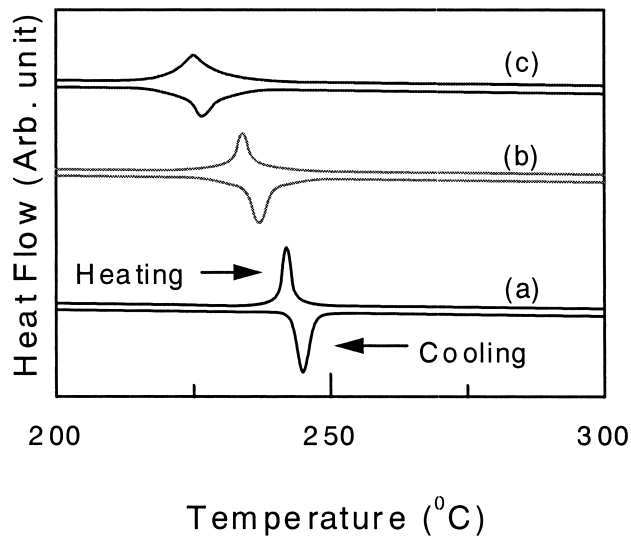


Fig. 4. Differential scanning calorimetric (DSC) curves of the  $\text{Mg}_2\text{Ni}$  system: (a) initial alloy, and recovered from (b) 6 GPa, (c) 6 GPa and 400°C.

and dehydrogenation, respectively. In the case of as-treated  $\text{Mg}_2\text{Ni}$ , such behaviour is strongly changed. The peaks owing to the hydride formation of  $\text{Mg}_2\text{NiH}_4$  and its thermal decomposition become broader and shift towards lower temperature than those observed for untreated sample. Since the phase structure is not changed after the pressure treatment, this result indicates that the absorption and desorption in DSC peaks are controlled by some kinetic factors such as the crystalline size and intergrain boundaries.

### 3.3. Effects of high-pressure of $\text{Mg}_2\text{NiH}_4$ on XRD and TG/DTA

Fig. 5 gives the XRD profiles of the initial  $\text{Mg}_2\text{NiH}_4$  and the treated ones. There exists little difference between initial  $\text{Mg}_2\text{NiH}_4$  (Fig. 5a) and that after high-pressure treatment only (Fig. 5b). However, obvious alternation was found in the profiles corresponding to the treated ones with heating. In particular, in the sample with heating the  $\text{LiAlH}_4$  (Fig. 5d), in addition to the shifts to lower 2-theta angles for most peaks, two new peaks marked by arrows were observed at  $42.72^\circ$  ( $d=2.1148 \text{ \AA}$ ) and  $62.08^\circ$  ( $d=1.4938 \text{ \AA}$ ). It is noted that the recovered phase with these two peaks is not stable when storing it at ambient temperature because these two peaks could not be detected even in a repeated measurement. Therefore, this should result from the quenching process of the high pressure and high temperature phase.

Fig. 6 illustrates the TG analyses of the hydride samples with different treating conditions. The dehydrogenating reactions for all the samples are fully completed below 400°C. With the high-pressure treatment and heating, the starting temperatures of dehydrogenating reactions reduced to

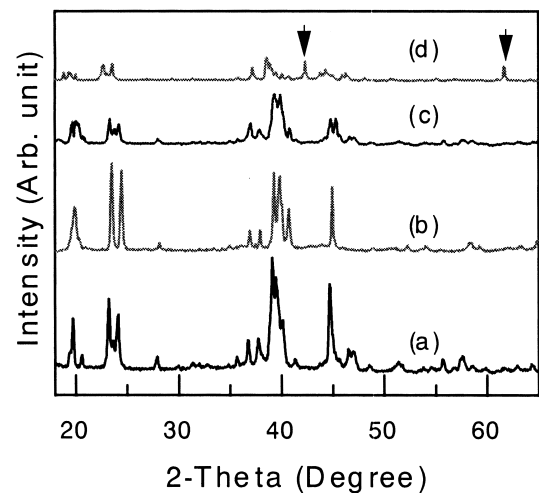


Fig. 5. X-ray diffraction (XRD) patterns of the hydride phases: (a) initial  $\text{Mg}_2\text{NiH}_4$ , and after recovery from (b) 6 GPa, (c) 6 GPa and 400°C, (d) 6 GPa and 400°C with  $\text{LiAlH}_4$ .

lower temperatures. However, it is worth noting that the total hydrogen content reaches nearly 4.3 wt.% for the sample with heating  $\text{LiAlH}_4$ , which exhibits three obvious regions for hydrogen desorption. These three desorption processes can be confirmed from the three enthalpic changes observed in DTA curves, as shown in Fig. 7. It is found that in addition to the two endotherms similar to that observed for the initial  $\text{Mg}_2\text{NiH}_4$ , a small and broad endotherm is also detected at 100°C, suggesting that there is a phase change due to the hydrogen desorption. The largest endotherm at 210°C and the small one at 320°C correspond to the decomposition of  $\text{Mg}_2\text{NiH}_4$  as well as the small amount of  $\text{MgH}_2$ . After the hydrogen desorption at 400°C, the XRD pattern of this sample (not shown in the present study) is consistent with the hexagonal structure of  $\text{Mg}_2\text{Ni}$ , as listed in the JCPDS Card No. 35-1225 [11]. It is known that normal  $\text{Mg}_2\text{NiH}_4$  contains interstitial hydride  $\text{Mg}_2\text{NiH}_{0.3}$  and complex hydride  $2\text{Mg}^{2+}[\text{NiH}_4]^{4-}$  [12–14]. After high pressure with heating treatment, the complex hydride would be the same, but the content of interstitial hydride increased from 0.3H to 1.6H [15]. Such a high hydrogen content may cause additional peaks on

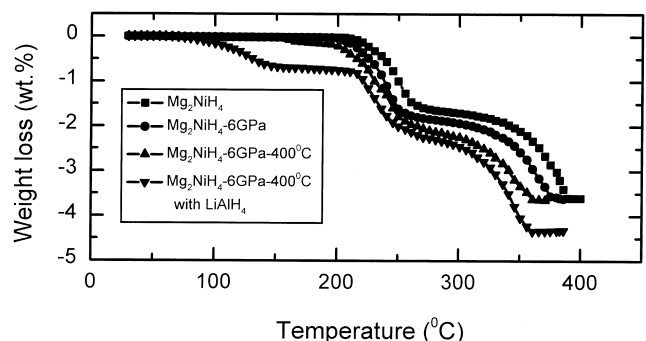


Fig. 6. Thermogravimetric (TG) profiles of the  $\text{Mg}_2\text{NiH}_4\text{-H}$  system.

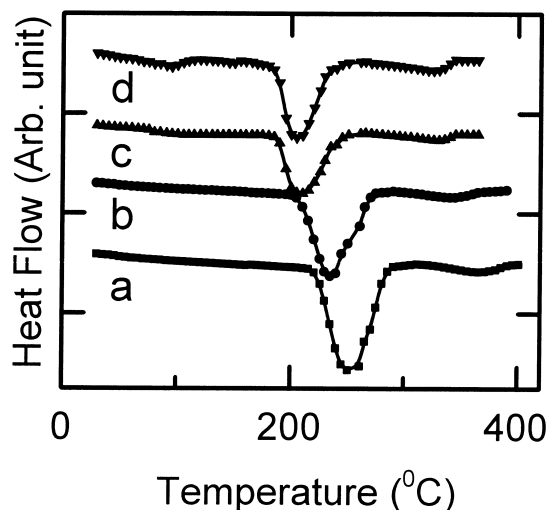


Fig. 7. Differential thermal analyses (DTA) of the  $\text{Mg}_2\text{NiH}_4\text{-H}$  system: (a) initial  $\text{Mg}_2\text{NiH}_4$ , and after recovery from (b) 6 GPa, (c) 6 GPa and 400°C, (d) 6 GPa and 400°C with  $\text{LiAlH}_4$ .

XRD pattern due to super lattice structure that can desorb hydrogen at lower temperature range.

#### 4. Conclusions

High pressure and heating treatment can be applied to the  $\text{Mg}_2\text{Ni}$  and  $\text{Mg}_2\text{NiH}_4$  systems, and it is very effective in improving the hydriding/dehydriding properties. It is concluded that high-pressure compression leads to the formation of a highly conductive alloy/hydride. Such a high-pressure operation, particularly on the  $\text{Mg}_2\text{NiH}_4$  with heating the hydrogen source  $\text{LiAlH}_4$ , reveals some profound implications since the hydride phase recovered from high pressure and high temperature can retain exceptionally higher hydrogen content with lower decomposition temperature. Its further study would lead to better and more practical hydrogen storage for the  $\text{Mg}_2\text{Ni}$  system.

#### Acknowledgements

This work was partially supported by a Grant-in-Aid for Special-Area Research from the Ministry of Education, Science and Culture (Japan). One of the authors (J. Chen) also acknowledges the research fellowship from New Energy and Industrial Technology Development Organization (NEDO) under the Ministry of International Trade and Industry of Japan.

#### References

- [1] B. Baranowski, in: G. Alefeld, J. Völkl (Eds.), *Hydrogen in Metals II*, Springer, Berlin, 1978, p. 157.
- [2] B. Baranowski, in: R. Pucci, G. Piccitto (Eds.), *Molecular Systems Under High Pressure*, Elsevier, Amsterdam, 1991, p. 139.
- [3] Y. Fukai, in: *The Hydrogen-metal System*, Springer, Berlin, 1993.
- [4] Y. Fukai, N. Okuma, *Jpn. J. Appl. Phys.* 32 (1993) L1256.
- [5] Y. Fukai, M. Yamakata, T. Yagi, *Z. Phys. Chem. Bd.* 179 (1993) 119.
- [6] Y. Fukai, N. Okuma, *Phys. Rev. Lett.* 73 (1994) 1640.
- [7] D.S. dos Santos, S. Miraglia, D. Fruchart, *J. Alloys Comp.* 291 (1999) L1.
- [8] Z. Gavra, G. Kimmel, Y. Gefen, M.H. Mintz, *J. Appl. Phys.* 57 (1985) 4548.
- [9] J. Chen, T. Sakai, N. Kitamura, H. Tanaka, H.T. Takeshita, N. Kuriyama, D. Harimoto, H. Nagai, Y. Fukai, *J. Alloys Comp.* 307 (2000) L1.
- [10] Y. Nakamura, K. Oguro, I. Uehara, E. Akiba, *Int. J. Hydrogen Energy* 25 (2000) 531.
- [11] JCPDS Card No. 35-1225 ( $\text{Mg}_2\text{Ni}$ ), JCPDS-ICDD, Newtown Square, PA 19073, 1999.
- [12] J.J. Reilly, R.H. Wiswall Jr., *Inorg. Chem.* 7 (1968) 2254.
- [13] J. Schefer, P. Fischer, W. Hälg, F. Stucki, L. Schlapbach, J.J. Didisheim, K. Yvon, *J. Less-Common Met.* 74 (1980) 65.
- [14] D. Noréus, L.G. Olsson, *J. Chem. Phys.* 78 (1983) 2419.
- [15] S. Orimo, H. Fujii, K. Ikeda, *Acta Mater.* 45 (1997) 331.